[1]Yue Liu*

Graph Neural Networks optimized with Gazelle Optimization Algorithm for Urban Plantscape Design Based on Large-scale Street View

Journal of Electrical Systems

Abstract: - The center of human activity and a key point of contact for social interaction between city people and the built environment is the street. With more street-level photos becoming available, urban landscape studies have more chances to examine and evaluate streetscapes closely and from various angles. This manuscript present the graph neural networks (GNN) optimized with gazelle optimization algorithm (GOA) for urban plants cape design based on large-scale street view (UPLS-GNN-GOA). Initially data is taken from ADE20K dataset. Afterward the data is fed to General Robust Subband Adaptive Filtering (GRSAF) based pre-processing process. The pre-processing output is given to Discrete Fractional Fourier Transforms (DFrFT) to extract the street greenery and openness of street canyons. After that, the extracted features are fed to Graph Neural Networks (GNN) to classify the public health, urban microclimate, human perception. The weight parameters of the GNN are optimized using Gazelle Optimization Algorithm (GOA).The UPLS-GNN-GOA method is implemented in Python, and its efficiency is determined using a series of performance evaluation metrics analysis, including accuracy, precision, recall, f1-score, and sensitivity. The proposed UPLS-GNN-GOA method shows the highest accuracy of 98%, precision of 98%, and F1-score of 97% while comparing other existing methods such as urban plantscape design based on convolutional neural network (UPLS-CNN), urban plantscape design based on deep convolutional neural network (UPLS-DCNN) and urban plantscape design based on deep learning and convolutional neural network (UPLS-DL-CNN) respectively.

Keywords: Graph Neural Network, Gazelle Optimization Algorithm, Large-Scale, Environment, Deep Learning, Urban Plantscape.

I. INTRODUCTION

Plantscaping deals with designing indoor spaces and interiors [1].Using deep learning and large-scale street views, urban plantscape design is an innovative approach that combines technology and urban planning principles to create sustainable and aesthetically pleasing urban environments [2]. This approach utilizes the abundance of street view images that are accessible and make use of deep learning techniques to analyze and understand the existing urban landscape [3].The term "constructed environment" refers to an artificial setting that include features of the constructed surroundings, such as the mixture of land usages, the density and intensity of buildings, the scale and articulation of streets, and the aesthetics of urban landscapes [4]. A well-designed urban environment helps to encourage outdoor activities, which in turn reduces the prevalence of many chronic illnesses and enhances psychological stress reduction, physical fitness, mental clarity, and the management of negative emotions [5, 6]. Numerous scholars from diverse disciplines have endeavored to quantify the perceived psychological strain experienced by urban dwellers within a constructed environment [7]. The most widely used method is to use questionnaires to assess psychological stress since conventional questionnaire designs are based on a range of psychological theories [8]. These techniques are time-consuming, expensive, and in-effective, Consequently, they are inappropriate for routinely measuring psychological stress [9]. They can, however, gauge the psychological stress that people perceive in a constructed setting. Moreover, their sample size is limited, making them unsuitable for large-scale constructed environments and only appropriate for small-scale investigations [10]. Furthermore, deep learning is being used more and more frequently because to the quick advancement of computer technology [11]. As a result, more academics are utilizing deep learning to investigate the constructed environment of cities and comprehend street quality [12]. In order to manage urban style, revitalize and transform established communities, and guide the development of new urban architectural styles, it is imperative to construct comprehensive architectural style databases [13]. Numerous cities have established control standards for architectural styles, resources found in landscape gardens, cultural sites, and other landscape-related components [14].

Continuity, progress, and regionalism are traits of urban architectural style [15]. Nonetheless, the objective, quick, and precise assessment of architectural style has consistently been a study challenge in the fields of urban planning and architecture [16]. Through the application of multiple linear regression analysis, the relationship between subjective psychological stress and the visual components of the urban built environment is evaluated [17].

[1*]Associate Professor, College of Information Engineering, Fuyang Normal University, Fuyang, Anhui, 236041, China
*Corresponding author e-mail: 200707011@fynu.edu.cn

Good and poor elements have been identified [18] as impacting the purported psychological strain.This deep learning-based analysis of massive data from street views can help planners and researchers gain more precise insights into how people interpret urban streets, which can lead to higher-quality urban planning [19]. When applied to the ADE20K dataset, a set of metrics is utilized to assess performance with regard to these shifts in geographic distribution and illustrate the advantages and disadvantages of common deep learning models [20].

In urban studies, the urban physical environment has been modelled and measured using a range of techniques and data sources. Street vegetation, urban shape, and urban environment modeling, for instance, have all been studied using high spatial resolution remotely sensed data and digital city models. Not every study can use these two kinds of techniques, though. The natural urban landscapes are typically neglected and the urban environment is oversimplified in digital city simulations. Furthermore, the profile view of plantscapes that people on the ground feel and sense is not represented in the overhead-view remotely sensed data. Street-level photos offer new possibilities for extremely fine-grained urban landscape studies from the perspective of the ground since they depict the plantscape's look and have a view angle comparable to that of pedestrians.

A. Contribution Statement

- Predicting urban plantscape using graph neural networks optimized with the gazelle optimization algorithm (UPLS-GNN-GOA).
- The data’s are gathered from the ADE20K dataset. Then the data’s are fed to pre-processing.
- Using a General Robust Subband Adaptive Filtering creates plantscape data in the pre-processing segment.
- The pre-processing output is fed into Discrete Fractional Fourier Transforms for extracting texture features.
- The extracted features are fed to Graph Neural Network, it classify the urban plantscape such as public health, urban microclimate, and human perception.
- The performance of the proposed approach is validated through python platform and compared with other existing techniques.
- After implementing the proposed UPLS-GNN-GOA technique, performance metrics including F1-score, accuracy, precision, recall, and sensitivity are examined.

The remaining portions of this paper are ordered as: sector 2 examines a survey of the works; sector 3 explains the proposed approach; sector4 gives the results and discussion; and sector5 concludes.

II. RECENT RESEARCH

In this section, some of the most recent studies on urban plantscape design based on deep learning and large-scale street views were evaluated.

Li et al. [21] have demonstrated how deep learning and large-scale street views are used in the design of urban plantscapes. A recently developed Deep Convolutional Neural Network program was showcased, which uses street-level pictures to analyze landscapes. A trained Deep CNN model successfully distinguished between several urban features from street-level photos. Artificial intelligence in conjunction with the vast collection of street-level photos offers a fresh perspective for urban landscape research in cities all over the world.

Stubbings et al. [22] have demonstrated how deep learning and large-scale street views are used in the design of urban plantscapes. Their approach involves utilizing a computer vision technique combined to create an index of urban street tree vegetation by employing a multilayer hierarchical model. that measures the quantity of vegetation perceptible from a pedestrian's perspective. We take two steps in our process. First, a cutting-edge DNN model was used to identify vegetated patches in street-level pictures. Second, a hierarchical multilevel model was used to incorporate data from multiple photos to provide an aggregated indication at the area level.

Wang et al. [23] have demonstrated how deep learning and large-scale street views are used in the design of urban plantscapes. While space syntax can theoretically support more comprehensive studies of street spatial perception, the growth of big data and computation has created new technological opportunities for measuring street perception quantitatively. Our research provides a novel approach to large-scale quality assessment of street spaces based on users' perceptions of the area. The area's street photos were used to build a deep learning scoring model.

Middel et al. [24] have demonstrated how deep learning and large-scale street views are used in the design of urban plantscapes. Using Google Street View (GSV) imagery, an inventive big data approach was devised to

determine the morphology of street views and the composition of urban features as experienced by pedestrians. Next, by assigning the training label to a void class and distinguishing between the three view orientations (lateral, down, and up), the classification accuracy was increased. Using partitioned picture cubes projected onto spheres, The street canyon's urban surroundings as perceived by a pedestrian were recreated, and the percentage of each surface class on the sphere was calculated.

Xu et al. [25] have demonstrated the deep learning- and large-scale street view-based urban plantscape design. Urban sensing and design strongly depended on the spatial distribution and visual quality of architectural kinds, which reflect the image of a city, influence people's daily lives, and can have good or negative social effects. Traditionally, architectural style identification has relied on human labor and has often been labor-intensive, wasteful, and subjective. The management of urban architectural styles on a big scale is greatly impacted by these concerns. Thankfully, deep learning models have proven to be very competitive in object detection recently and possess strong feature expression capabilities for photos. They offer a fresh method for assisting with the identification of conventional architectural styles.

Kim and Lee [26] have demonstrated the urban plantscape design that is based on deep learning and large-scale street views. This research presents a method using reference photos and a deep learning model to discover and append interior design style information stochastically. Design style was a helpful notion in the field of interior design and has been crucial in assisting people in comprehending and communicating interior design. The study then focuses on the application of a data-driven, deep learning-based technique to stochastically identify the design style of given reference pictures for interior design.

XIA et al. [27] have demonstrated the urban plantscape design that is based on deep learning and large-scale street views. The presence of street vegetation is directly linked to people's physical and emotional well-being and has long been considered essential to the quality of urban landscapes. Researchers mimic and quantify urban greenery using a variety of techniques in their current study on the urban environment. The image provided by Google Street View resembled the one taken from a pedestrian's point of view. It was more suited for researching greening of urban streets. With the advancement of deep learning-based artificial intelligence, we can do away with laborious manual statistical work and extract more precise semantic information from street photos. Also has the capacity to assess green spaces in greater city regions and to gather additional information from street view photos for urban studies.

III. PROPOSED METHODOLOGY

The proposed UPLS-GNN-GOA is discussed in this section. This section presents the clear description about the research methodology for urban plantscape recommendation. First, the ADE20K dataset is used to obtain the input images. The block schematic of the proposed UPLS-GNN-GOA technique is represented in Fig 1. Thus, the detailed description about UPLS-GNN-GOA is given below,

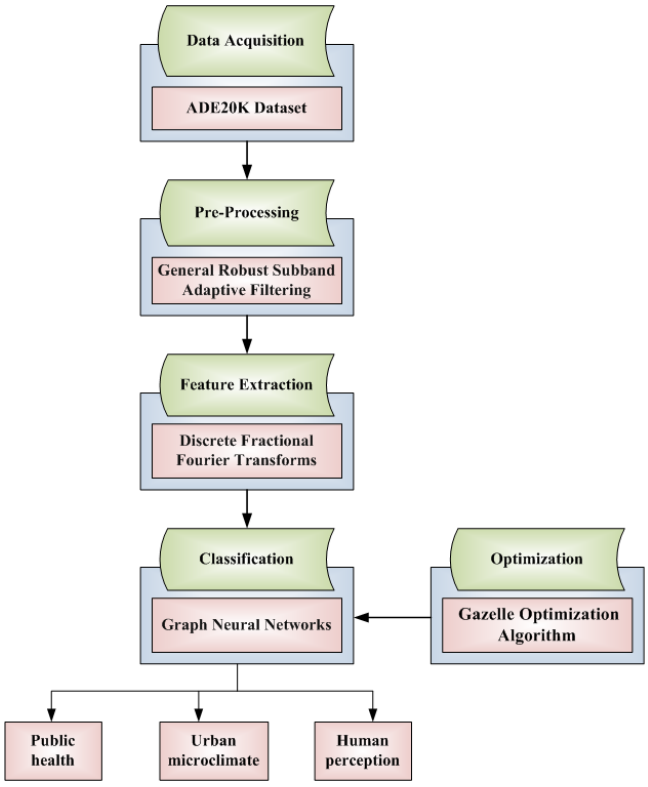

Fig 1: Block schematic of the proposed UPLS-GNN-GOA technique

A. Data Collection

Specifically, the training set has 20,210 images, the testing set contains 3,000, and the validation set contains 2,000 images [28]. 3,169 class labels have been annotated in total; of them, 476 are object part classes and 2,693 are object and stuff classes. Every image has a thorough object annotation. The parts of many things are also annotated. There is more information about each object, including various qualities and information on whether it is cropped or obscured. While the part annotations are not exhaustive over the photos in the training set, they are exhaustive over the images in the validation set.

B. Pre-Processing Using General Robust Subband Adaptive Filtering

In this phase, general robust subband adaptive filtering (GRSAF) pre-processes the input data, which is utilized for urban plantscapein the dataset [29].In order to enhance the cleanliness of the data, we employed the general robust subband adaptive filtering (GRSAF).We will examine an issue with system identification in which the pair of data between input and output $\{u(n), d(n)\}$ obeys the following relation at every time index n:

$$d(n) = u^T(n)w^0 + v(n), \tag{1}$$

Here the input vector $u(n) = [u(n), u(n-1), ..., u(n-M\_+1)]^T$ is denoted as M-dimensional and is not affected by the additive noise $v(n)$, and $(.)^T$ stands for transposition. The identical input signal $u(n)$ must be sent through an adaptive filter $w(n)$ in order to estimate the unknown system's impulse response, which is represented by the $M \times 1$ vector w^0. The vector of weight $w(k)$, which is obtained from the decimated subband error signals, provides the estimation of w^0 in the decimated sequences.

$$e_i, D(k) = d_i, D(k) - y_i, D(k) \tag{2}$$

$$e_i, D(k) = d_i, D(k) - u_i^T(k)w(k-1), \tag{3}$$

For $i = 0, \ldots, N-1.$

In certain real-world scenarios, like the EC, We may concentrate on the error in the output $e(n)$ in the initial classifications. We therefore copy $w(k)$ to $w(n)$ for each of the input samples (N).

Besides Gaussian noise, the additive noise could also include impulsive noise. M-NSAF algorithm is described as follows for updating the weight vector, hence offering robustness against abrupt noise:

$$w(k) = w(k-1) + \mu \sum_{i=0}^{N-1} \frac{\varphi'(e_i, D(k))u_i(k)}{\|u_i(k)\|} \tag{4}$$

Here μ > 0 is denoted asthe magnitude of the steps and || • ||2 indicates a vector's l_2 norm. The function that determines the score is provided by

$$\varphi'(x) \triangleq \frac{\partial \varphi(x)}{\partial x} = \begin{Bmatrix} x, if|x| < \xi \\ 0, if|x| \geq \xi \end{Bmatrix} \tag{5}$$

And ξ is a threshold parameter.

When $|e_i, D(k)| < \xi$ holds, it reduces to the traditional NSAF method using M-NSAF algorithm. To ensure the method's stability, the weight vector's adaptation will be terminated by the M-NSAF algorithm once $|e_i D(k)|$ values exceed ξ.

Derivation of Update: First, we can reorder (4) as follows:

$$w(k) = w(k-1) + \sum_{i=0}^{N-1} q(e_{i,} D(k)) g_i(k) e_i, D(k), \tag{6}$$

Where

$$q(x) \triangleq \frac{\varphi'(x)}{x} = \begin{Bmatrix} 1, if|x| < \xi \\ 0, if|x| \geq \xi \end{Bmatrix}, \tag{7}$$

In order to proceed, in the decimated domain, we assume that the random-walk model produces the unknown vector w^0.

$$w^0(k) = w^0(k-1) + c(k), \tag{8}$$

A universal structure for the scaling factor and the sturdy SAF $q(e_i, D(k))$ is presented. Specifically, using an alternative robust cost function $\varphi(e_{i,} D(k))$, we can directly calculate $q(e_{i,} D(k)) = \frac{1}{\sqrt{2\pi}\beta}\left[1 - \exp\left(-\frac{e_i^2, D(k)}{2\kappa_\sigma^2}\right)\right]$ which leads to

$$q(e_{i,} D(k)) = \exp\left(-\frac{e_i^2, D(k)}{2\kappa_\sigma^2}\right), \tag{9}$$

The kernel width is denoted by $\kappa_\sigma > 0$. Like the previously described modified Huber criterion, GR-SAF, which is based on MCC, provides robustness against impulsive noise since $q(e_i, D(k))$, when impulsive noise happens, the result of the MCC criterion will be close to 0. Next, the weight update is produced as

$$w(k) = w(k-1) + \sum_{i=0}^{N-1} \frac{q(e_i, D(k))u_i(k)e_i, D(k)}{\|u_i(k)\| + \frac{\sigma_{v,i}^2}{\sigma_\Phi^2(k-1)}} \tag{10}$$

At a glance, the scaling parameter $q(e_i, D(k))$ contributes to resilience against impulsive noise. $\sigma_\Phi^2(k)$ will eventually get extremely little as the method converges, which will cause $\delta(k)$ to grow very large and ultimately result in minimal steady-state estimation error.

Thus this method removes the noise from the input data. Finally, the pre-processed output is given towards feature extraction.

C. Feature Extraction Using Discrete Fractional Fourier Transform(DFrFT)

In this section, For feature extraction, the pre-processed data are submitted to the DFrFT. With the inclusion of a single fractional parameter, regular discrete transforms are expanded into discrete fractional transforms [31]. Similar to the discrete Fourier transform, discrete fractional transforms have been introduced and have

been discovered to have many applications in a wide range of scientific and technological sectors. The discrete analogue of the integral FrFT, or DFrFT, is one well-known example. The DFrFT is not only appropriate from a numerical perspective, but it has also shown to be an effective signal processing technique throughout time. Currently, there are many definitions of DFrFT available. The first approach is represented by direct sampling of the FrFT. This kind of DFrFT can be computed using several different algorithms, and it is the simplest method available. However, the FrFT's unitarily, reversibly, and additively features could be lost in these discrete realizations, which would limit the applicability of the function. A different approach is based on linearly mixing ordinary Fourier operators increased to different powers.

Using a spectral expansion in certain eigenvectors that make up the discrete analogue of the set of Hermit-Gaussian functions DFrFT was developed. These are the well-known DFT Eigen functions.

$$Y_{N\times 1} = F_N^{\alpha} X_{N\times 1} \tag{11}$$

Here, F_N^{α} is $(N\times N)$matrix for the fractional Fourier transform in discrete order, $X_{N\times 1} = [x_0, x_1, ..., x_{N-1}]^T$ and $Y_{N\times 1} = [y_0, y_1, ..., y_{N-1}]^T$ are vectors of data for input and output, correspondingly, and α is a parameter with fractions.

Any matrix, including the DFT matrix, can have its fractional power found using the power of eigenvalues and the matrix's eigenvalue decomposition:

$$F_N^{\alpha} = Z_N \Lambda_N^{\alpha} Z_N^T \tag{12}$$

Where, Λ_N^{α} is denoted as a size N diagonal matrix whose diagonal entries are the eigenvalues' exponent powers in the DFT matrix, and Z_N is a matrix with the normalized mutually orthogonal eigenvectors of the DFT matrix as its columns.

We can characterize the DFrFT matrix's entries as follows based on those broad considerations:

$$F_N^{\alpha} = \begin{bmatrix} f_{0,0}^{(\alpha)} & f_{0,1}^{(\alpha)} & \cdots & f_{0,1}^{(\alpha)} \\ f_{0,1}^{(\alpha)} & f_{1,1}^{(\alpha)} & \cdots & f_{1,N-1}^{(\alpha)} \\ \cdots & \cdots & \cdots & \cdots \\ f_{0,1}^{(\alpha)} & f_{1,N-1}^{(\alpha)} & \cdots & f_{1,1}^{(\alpha)} \end{bmatrix} \tag{13}$$

The values of the complex numbers that make up this matrix's entries are determined by the fractional parameter as well as the number N. Nonetheless, it will be more practical for us to use the letters of the common Latin alphabet $\{a_N^{(\alpha)}, b_N^{(\alpha)}, c_N^{(\alpha)}, ..., z_N^{(\alpha)}\}$ to represent the matrix constituents' numerical values. In this instance, the fractional parameter's value is indicated by the superscript, while the subscript N denotes the size of the DFrFT matrix. This will make it easier to identify the matrix's structural characteristics and determine whether compositions with identical entry values exist inside it.

Computing the Two-Point DFrFT

Let $X_{2\times 1} = [x_0, x_1]^T$ and $Y_{2\times 1} = [y_0, y_1]^T$ be the input and output data vectors in two dimensions, correspondingly.

$$Y_{2\times 1} = F_2^{\alpha} X_{2\times 1} \tag{14}$$

Computing the Three-Point DFrFT

Let $X_{3\times 1} = [x_0, x_1, x_2]^T$ and $Y_{3\times 1} = [y_0, y_1, y_2]^T$ be the input and output data vectors in three dimensions, correspondingly.

The following form can be used to represent the three-point DFrFT:

$$Y_{3\times 1} = F_3^{\alpha} X_{3\times 1} \tag{15}$$

The extracted features are environment and plants variations. Then the extracted output is given to classification phase.

D. Classification using Graph Neural Networks (GNN)

This part [30] covered the classification of real-time interaction of urban plantscape using GNN. For machine learning, graph analysis is a unique type of non-Euclidean data structure that is utilized for clustering,

link prediction, and node classification. Deep learning techniques that operate in the graph domain are called GNNs. Because of its compelling outcomes, GNN has recently gained popularity as a graph analysis method. We shall demonstrate the underlying reasons of graph neural networks in the ensuing paragraphs.

When using spectral approaches, a graph signal x is first converted by the graph Fourier transforms f to the spectral domain, and then the convolution operation is carried out.

$$f(x) = U^T x \tag{16}$$

$$f^{-1}(x) = Ux \tag{17}$$

Here U is denoted as the Laplacian normalized graph's eigenvector matrix.

On the basis of the graph's topology, spatial techniques define convolutions directly on it. Determining the convolution process with varying neighborhood sizes and preserving CNN local invariance are the primary problems with spatial techniques.

$$t = h_v^t + \sum_{u \in N_w} h_u^t \tag{18}$$

$$h_v^{t+1} = \sigma\left(tW_{|N_v|}^{t+1}\right) \tag{19}$$

Where $W_{|N_v|}^{t+1}$ is the weight matrix pertaining to degree nodes $|N_v|$ at layer t+1.

Three categories are used to group the GNN applications: structural, non-structural, and other. We then provide a thorough analysis of the applications in each category.

The optimal signal is predicted by proposed GNN technique. Finally, the GNN classifies public health, urban microclimate, and human perception.

E. Optimization using GOA

The ideal parameters of the GNN classifier are optimized using the GOA [31]. The ability of gazelles to survive in their environment when predators predominate served as the inspiration for this article. The gazelle knows every day that it will be dinner for the day if it cannot outrun and outsmart its predators. They are not considered endangered because, despite their low status in the food chain, they appear to be doing something healthy. Avoiding predators is one of those morally good actions performed by gazelles.

Step 1: Initialization

The GNN's starting weight parameter

***Step 2*:** Random Generation

Following initialization, the random vectors produce the input parameters at random.

$$X = \begin{bmatrix} X_{1,1} & X_{1,2} & \cdots & X_{1,d} \\ X_{2,1} & X_{2,2} & \cdots & X_{2,d} \\ \cdots & \cdots & \cdots & \cdots \\ X_{n,1} & X_{n,2} & \cdots & X_{n,d} \end{bmatrix} \tag{20}$$

Here X denotes the GOA population matrix, n is indicated as the amount of lyrebirds, and d is denoted as the count of decision variables, respectively.

Step 3: Fitness Calculation

From initialized assessments, random solution is produced. It is expressed in equation

$$F = Optimize[W]$$

Step 4: Exploitation phase

In this stage, it is assumed that the gazelles are either stalked by a predator or are grazing contentedly in the absence of one. During this stage, we efficiently covered the domain's surrounding territories by using Brownian motion, which is distinguished by steady, predictable steps. The mathematical model of this behavior is represented by equation.

$$\overrightarrow{gazelle_{t+1}} = \overrightarrow{gazelle_t} + s.\vec{R} * .\vec{R}_B * .\left(\overrightarrow{Elite_i} - \vec{R}_B * . \overrightarrow{gazelle_t}\right) \tag{21}$$

Where $\overrightarrow{gazelle_{t+1}}$ is represent as the next iteration's solution, $\overrightarrow{gazelle_t}$ is indicated as the current iteration's solution, S means the gazelles' rate of grazing, $\vec{R}_B$ is a vector that depicts the Brownian motion by using random numbers.

Step 5: Exploration phase

The exploring phase starts as soon as a predator is spotted. We set the 2 m height to a count between 0 and 1 in order to simulate the gazelles' response to danger. When jumping, gazelles will either stomp their feet, flick their tail, or use a technique called "stotting," in which they jump with all four feet up to a height of two meters. For this part of the algorithm, we used the Levy flight, which entails making small steps and sometimes large jumps. This method has been used in the optimization literature to enhance search capability.

Equation illustrates the mathematical model of the gazelle's behaviour after it detects a predator.

$$\overrightarrow{gazelle_{t+1}} = \overrightarrow{gazelle_t} + S.\mu.\vec{R} * .\vec{R}_L * .\left(\overrightarrow{Elite_i} - \vec{R}_L * . \overrightarrow{gazelle_t}\right) \tag{22}$$

If S is the maximum speed the gazelle may travel at, then $\vec{R}_L$ is indicated as a vector of random values drawn from Levy distributions.

Step 6: Termination Criteria

Verify the termination criteria; if it is met, the best possible solution has been found; if not, repeat the procedure. Use the optimized parameter values of the generator from GNN with the help of gazelle optimization algorithm. Analyze urban plantscape designs using deep learning and large-scale street views. Fig 2 shows that the Flowchart for GOA.

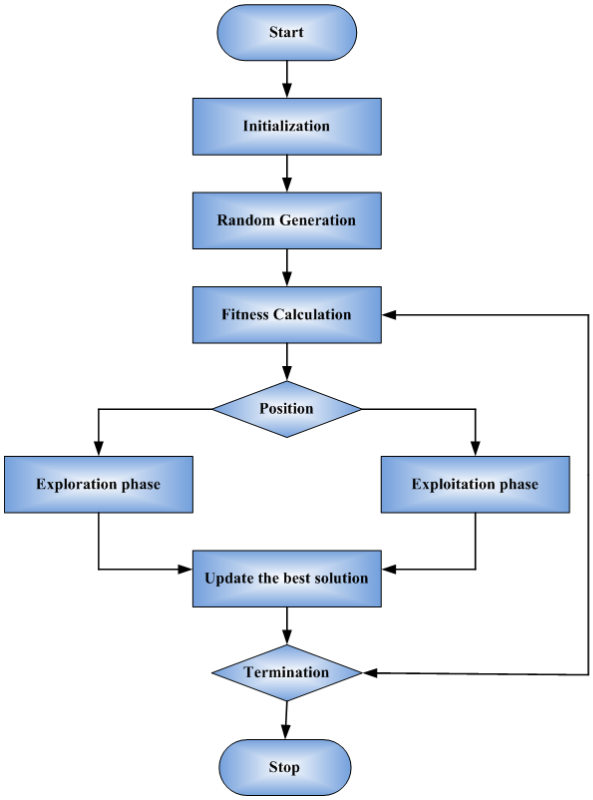

Fig 2: Flowchart for GOA

IV. RESULT AND DISCUSSION

This sector discusses the experimental outcomes of the proposed method. Next, Python is used to simulate the proposed approach using the specified performance metrics. The proposed UPLS-GNN-GOA approach is implemented in Python using ADE20K dataset. The obtained outcome of the proposed UPLS-GNN-GOA approach is analysed with existing systems like UPLS-DCNN, UPLS-CNN, and UPLS-DL-CNN respectively.

A. Performance Measures

In order to choose the optimal classifier, this is an important task. Performance indicators like recall, sensitivity, F1-score, accuracy, and precision are analyzed to assess performance. It is determined to scale the

performance measures using the confusion matrix. False Positive, False Negative, True Positive, and True Negative values are needed to scale the confusion matrix.

- True Positive (TP): The number of samples in which the actual class label matches exactly the one predicted, implying a positive outcome.
- True Negative (TN): The number of samples in which the actual class label matches exactly the predicted class label, implying a negative result.
- False Positive (FP): The number of samples in which the actual class label is imprecise while the predicted class label suggests a positive value.
- False Negative (FN): The number of samples in which the actual class label is imprecise and the predicted class label suggests a negative value.

1) Accuracy

It is the proportion of the entire count of predictions made for a dataset separated by the count of exact forecasts. It is quantified using eqn (23).

$$Accuracy = \frac{\left(TP + TN\right)}{\left(TP + FP + TN + FN\right)} \tag{23}$$

Where, TN s denoted as true negative, TP is represent as true positive, FP is indicated as false positive, and FN is signifies as false negative.

2) Precision (P)

A statistic called precision counts how many positive predictions were made correctly. Equation (24), used to scale this,

$$\Pr ecision = \frac{TP}{\left(TP + FP\right)} \tag{24}$$

3) F1 Score

The accuracy and precision weighted mean is called the F1-Score. Equation (25) is used to express it.

$$F1Score = \frac{TP_{\alpha}}{\left(TP_{\alpha} + \frac{1}{2}\left[FP_{\lambda} + FN_{\gamma}\right]\right)} \tag{25}$$

4) Recall

This is defined with the help of eqn (26)

$$\text{Re}call = \frac{\delta}{\delta + \lambda} \tag{26}$$

B. Performance Analysis

The simulation results of the proposed UPLS-GNN-GOA approach are shown in Fig 3 to 7. Next, the proposed UPLS-GNN-GOA approach is contrasted with the existing methods such as, UPLS-DCNN, UPLS-CNN, and UPLS-DL-CNN correspondingly.

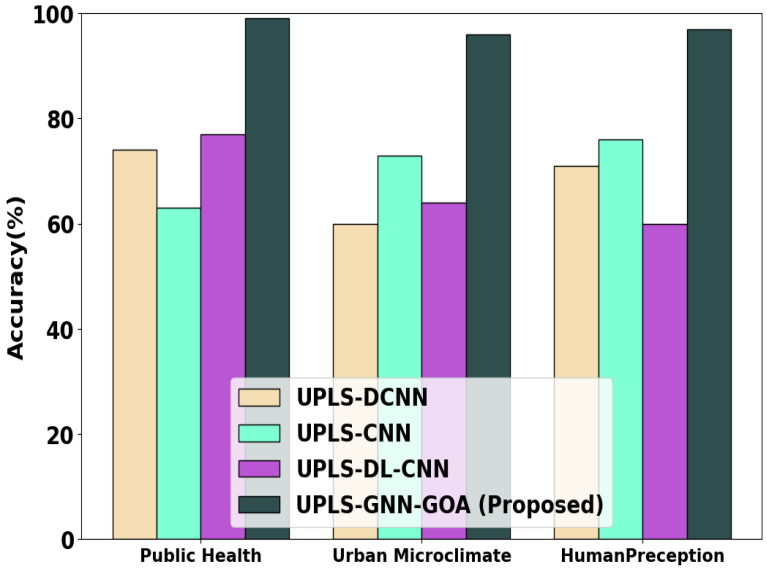

Fig 3: Performance analysis of accuracy

The performance analysis of accuracy is demonstrated in Fig 3. The performance of the proposed UPLS-GNN-GOA technique results in accuracy that are 35.98%, 28.56%, 41.27%, higher for the classification of Public health, 22.47%, 38.98%, 26.94%, higher for the classification of Urban microclimate and 25.47%, 30.86%, 21.48%, higher for the classification of Human perception when evaluated to the existing UPLS-DCNN, UPLS-CNN, and UPLS-DL-CNN models respectively.

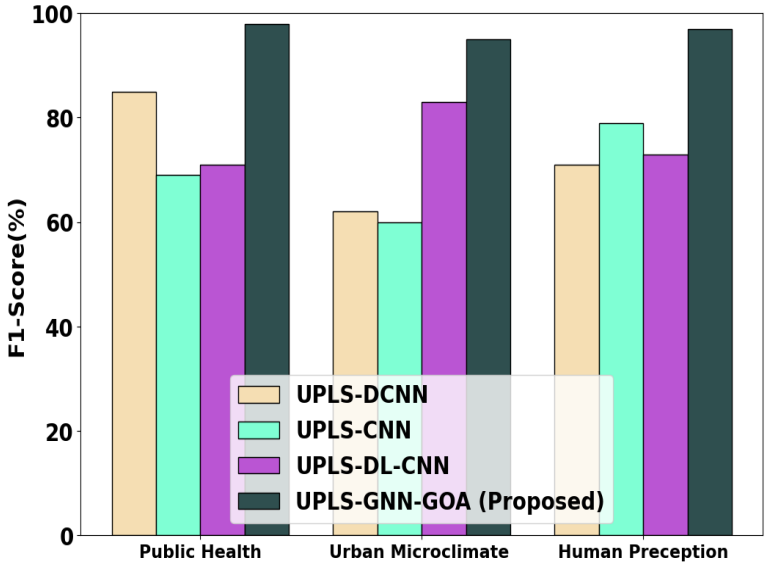

Fig 4: Analysis the performance of F1-score value

Analysis the performance of F1-score value with proposed method is illustrated in Fig 4. The performance of the proposed UPLS-GNN-GOA technique results in F1-score that are 35.71%, 26.59%, 29.24%, %, higher for the classification of Public health, 22.66%, 23.52%, 37.97%, higher for the classification of Urban microclimate and 21.45%, 28.96%, 25.85% higher for the classification of Human perception when evaluated to the existing UPLS-DCNN, UPLS-CNN, and UPLS-DL-CNN models correspondingly.

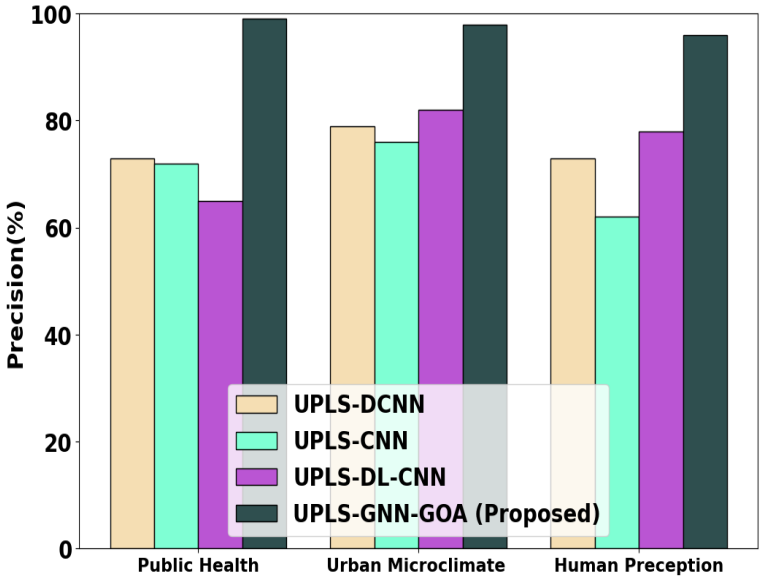

Fig 5: Comparison of precision value with proposed and existing method

The comparison of precision value with proposed and existing system is illustrated in Fig 5. Here, a direct comparison with proposed approaches is offered to show how the suggested method's precision is higher. The proposed method provides for a more extensive analysis of a proposed and has higher precision than existing methods due to its wider consideration of factors. The performance of the proposed UPLS-GNN-GOA technique results in precision that are 36.86%, 31.76%, 28.75%, higher for the classification of Public health, 27.86%, 24.96%, 31.84% higher for the classification of Urban microclimate and26.95%, 22.56%, 32.41% higher for the classification of Human perception where evaluated to the existing UPLS-DCNN, UPLS-CNN, and UPLS-DL-CNN models correspondingly.

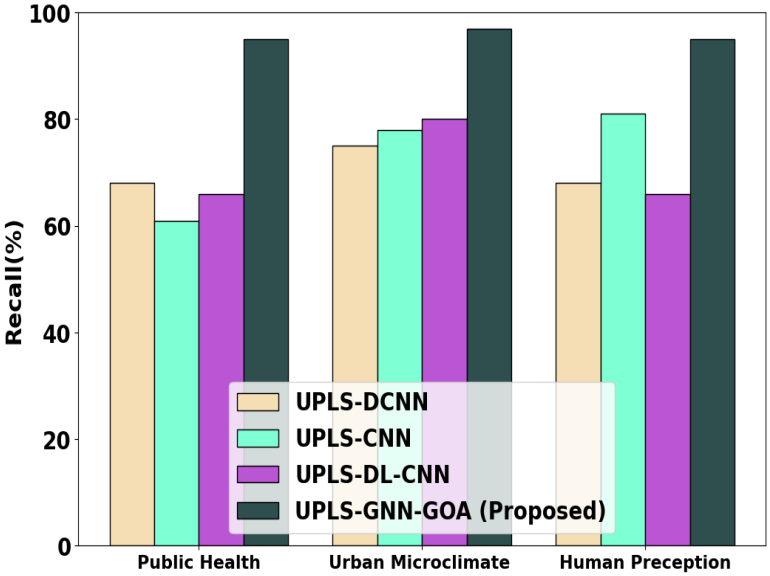

Fig 6: Comparison of recall value with proposed and existing method.

The comparison of recall value with proposed and existing system is illustrated in Fig 6. The performance of the proposed UPLS-GNN-GOA technique results in recall that are 29.76%, 21.91%, 25.47% higher for the classification of Public health, 21.76%, 23.46%, 26.92% higher for the classification of Urban microclimate and 24.47%, 31.93%, 21.88% higher for the classification of Human perception where evaluated to the existing UPLS-DCNN, UPLS-CNN and UPLS-DL-CNN models correspondingly.

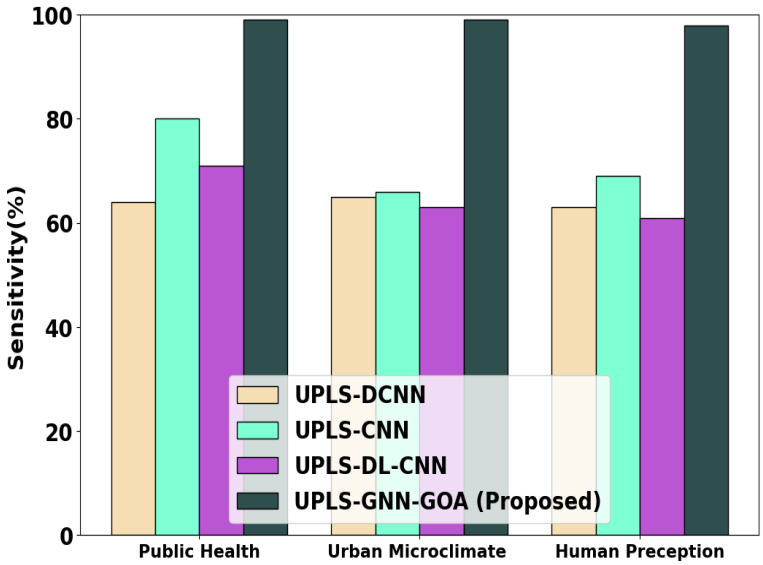

Fig 7: Comparison of sensitivity value with proposed and existing method

The comparison of sensitivity value with proposed and existing system is illustrated in Fig 7. The performance of the proposed UPLS-GNN-GOA technique results in sensitivity that are 21.94%, 32.57%, 28.27%, higher for the classification of Public health, 23.97%, 26.78%, 22.32% higher for the classification of Urban microclimate and 24.75%, 31.79%, 21.96% higher for the classification of Human perception where evaluated to the existing UPLS-DCNN, UPLS-CNN, and UPLS-DL-CNN models respectively.

V. CONCLUSION

In this section, urban plantscape design using UPLS-GNN-GOA method was successfully implemented for classifying public health, urban microclimate, and human perception. The proposed UPLS-GNN-GOA procedure is carried out using the Python platform with the dataset of GSV dataset. The performance of the UPLS-GNN-GOA method contains accuracy, precision, recall, F-score and sensitivity. The proposed UPLS-GNN-GOA method attains 98%, 98% and 97% higher accuracy for urban plantscape, respectively. The computational time performance of the proposed method attains 99sec, lower computation. The proposed UPLS-GNN-GOA method attains3%, 2% and 4% lower error rate of fashion styles. The proposed UPLS-GNN-GOA method attains 98%, 99% and 99% higher precision of fashion styles, respectively. The proposed UPLS-GNN-GOA method attains 99%, 98% and 97% higher recall of fashion styles, respectively. The proposed UPLS-GNN-GOA method attains 98%, 99% and 99% higher sensitivity of fashion styles, respectively. The proposed UPLS-GNN-GOA method attains 98%, 99% and 97% higher specificity of fashion styles, respectively. The effectiveness of the suggested UPLS-GNN-GOA approach is contrasted with the current approaches, including UPLS-CNN, UPLS-DCNN and UPLS-DL-CNN.

Acknowledgements

This research was funded by the Anhui Philosophy and Social Science Planning Youth Project in 2022 (Grant No :AHSKQ2022D173): A study on the inheritance and innovation of red cultural resources in Northern Anhui from the perspective of tourism landscape.

REFERENCES

[1] Wei, J., Yue, W., Li, M., & Gao, J. (2022). Mapping human perception of urban landscape from street-view images: A deep-learning approach. *International Journal of Applied Earth Observation and Geoinformation*, *112*, 102886.

[2] Zhong, T., Ye, C., Wang, Z., Tang, G., Zhang, W., & Ye, Y. (2021). City-scale mapping of urban façade color using street-view imagery. *Remote Sensing*, *13*(8), 1591.

[3] Verma, D., Mumm, O., & Carlow, V. M. (2021). Identifying Streetscape Features Using VHR Imagery and Deep Learning Applications. *Remote Sensing*, *13*(17), 3363.

[4] Biljecki, F., & Ito, K. (2021). Street view imagery in urban analytics and GIS: A review. *Landscape and Urban Planning*, *215*, 104217.

[5] Rui, Q., & Cheng, H. (2023). Quantifying the spatial quality of urban streets with open street view images: A case study of the main urban area of Fuzhou. *Ecological Indicators*, *156*, 111204.

[6] Zhao, T., Liang, X., Tu, W., Huang, Z., & Biljecki, F. (2023). Sensing urban soundscapes from street view imagery. *Computers, Environment and Urban Systems*, *99*, 101915.

[7] He, N., & Li, G. (2021). Urban neighbourhood environment assessment based on street view image processing: A review of research trends. *Environmental Challenges*, *4*, 100090.

[8] Tang, Z., Ye, Y., Jiang, Z., Fu, C., Huang, R., & Yao, D. (2020). A data-informed analytical approach to human-scale greenway planning: Integrating multi-sourced urban data with machine learning algorithms. *Urban Forestry & Urban Greening*, *56*, 126871.

[9] Zhang, J., & Hu, A. (2022). Analyzing green view index and green view index best path using Google street view and deep learning. *Journal of Computational Design and Engineering*, *9*(5), 2010-2023.

[10] Ta, D. T., & Furuya, K. (2022). Google Street View and Machine Learning—Useful Tools for a Street-Level Remote Survey: A Case Study in Ho Chi Minh, Vietnam and Ichikawa, Japan. *Land*, *11*(12), 2254.

[11] Lumnitz, S., Devisscher, T., Mayaud, J. R., Radic, V., Coops, N. C., & Griess, V. C. (2021). Mapping trees along urban street networks with deep learning and street-level imagery. *ISPRS Journal of Photogrammetry and Remote Sensing*, *175*, 144-157.

[12] Wang, R., Feng, Z., Pearce, J., Yao, Y., Li, X., & Liu, Y. (2021). The distribution of greenspace quantity and quality and their association with neighbourhood socioeconomic conditions in Guangzhou, China: A new approach using deep learning method and street view images. *Sustainable Cities and Society*, *66*, 102664.

[13] Kim, J. H., Lee, S., Hipp, J. R., & Ki, D. (2021). Decoding urban landscapes: Google street view and measurement sensitivity. *Computers, Environment and Urban Systems*, *88*, 101626.

[14] Zhang, J., Fukuda, T., & Yabuki, N. (2020, July). A large-scale measurement and quantitative analysis method of façade color in the urban street using deep learning. In *The International Conference on Computational Design and Robotic Fabrication* (pp. 93-102). Singapore: Springer Singapore.

[15] Wen, D., Liu, M., & Yu, Z. (2022). Quantifying ecological landscape quality of urban street by open street view images: A case study of xiamen island, china. *Remote Sensing*, *14*(14), 3360.

[16] Chen, C., Li, H., Luo, W., Xie, J., Yao, J., Wu, L., & Xia, Y. (2022). Predicting the effect of street environment on residents' mood states in large urban areas using machine learning and street view images. *Science of The Total Environment*, *816*, 151605.

[17] Tian, H., Han, Z., Xu, W., Liu, X., Qiu, W., & Li, W. (2021). Evolution of historical urban landscape with computer vision and machine learning: A case study of Berlin. *J. Digit. Landsc. Archit*, *6*, 436-451.

[18] Zhao, J., & Guo, Q. (2022). Intelligent assessment for visual quality of streets: exploration based on machine learning and large-scale street view data. *Sustainability*, *14*(13), 8166.

[19] Kruse, J., Kang, Y., Liu, Y. N., Zhang, F., & Gao, S. (2021). Places for play: Understanding human perception of playability in cities using street view images and deep learning. *Computers, Environment and Urban Systems*, *90*, 101693.

[20] Zhou, B., Zhao, H., Puig, X., Xiao, T., Fidler, S., Barriuso, A., & Torralba, A. (2019). Semantic understanding of scenes through the ade20k dataset. *International Journal of Computer Vision*, *127*, 302-321.

[21] Li, X., Cai, B. Y., & Ratti, C. (2018). Using street-level images and deep learning for urban landscape studies. *Landscape Architecture Frontiers*, *6*(2), 20-30.

[22] Stubbings, P., Peskett, J., Rowe, F., & Arribas-Bel, D. (2019). A hierarchical urban forest index using street-level imagery and deep learning. *Remote Sensing*, *11*(12), 1395.

[23] Wang, L., Han, X., He, J., & Jung, T. (2022). Measuring residents' perceptions of city streets to inform better street planning through deep learning and space syntax. *ISPRS Journal of Photogrammetry and Remote Sensing*, *190*, 215-230.

[24] Middel, A., Lukasczyk, J., Zakrzewski, S., Arnold, M., & Maciejewski, R. (2019). Urban form and composition of street canyons: A human-centric big data and deep learning approach. *Landscape and Urban Planning*, *183*, 122-132.

[25] Xu, H., Sun, H., Wang, L., Yu, X., & Li, T. (2023). Urban Architectural Style Recognition and Dataset Construction Method under Deep Learning of street View Images: A Case Study of Wuhan. *ISPRS International Journal of Geo-Information*, *12*(7), 264.

[26] Kim, J., & Lee, J. K. (2020). Stochastic detection of interior design styles using a deep-learning model for reference images. *Applied Sciences*, *10*(20), 7299.

[27] XIA, Y., YABUKI, N., & FUKUDA, T. SYSTEM BASED ON DEEP LEARNING AND GOOGLE STREET VIEW.

[28] Habibi, Z. A. H. R. A., Zayyani, H. A. D. I., & Abadi, M. S. E. (2021). A robust subband adaptive filter algorithm for sparse and block-sparse systems identification. *Journal of Systems Engineering and Electronics*, *32*(2), 487-497.

[29] Zhou, J., Cui, G., Hu, S., Zhang, Z., Yang, C., Liu, Z., ... & Sun, M. (2020). Graph neural networks: A review of methods and applications. *AI open*, *1*, 57-81.

[30] Bispo, B. C., de Oliveira Neto, J. R., & Lima, J. B. (2024). Hardware Architectures for Computing Eigendecomposition-Based Discrete Fractional Fourier Transforms with Reduced Arithmetic Complexity. *Circuits, Systems, and Signal Processing*, *43*(1), 593-614.

[31] Agushaka, J. O., Ezugwu, A. E., & Abualigah, L. (2023). Gazelle optimization algorithm: a novel nature-inspired metaheuristic optimizer. *Neural Computing and Applications*, *35*(5), 4099-4131.